Phase Diagrams for Ceramists
1969 Supplement

Ernest M. Levin,
Carl R. Robbins and
Howard F. McMurdie

Compiled at the National Bureau of Standards

Margie K. Reser, *Editor*

SECOND PRINTING 1985

The American Ceramic Society
65 Ceramic Drive, Columbus, Ohio 43214

Printed in U.S.A.

ISBN 0-916094-05-7

Al_2O_3–La_2O_3

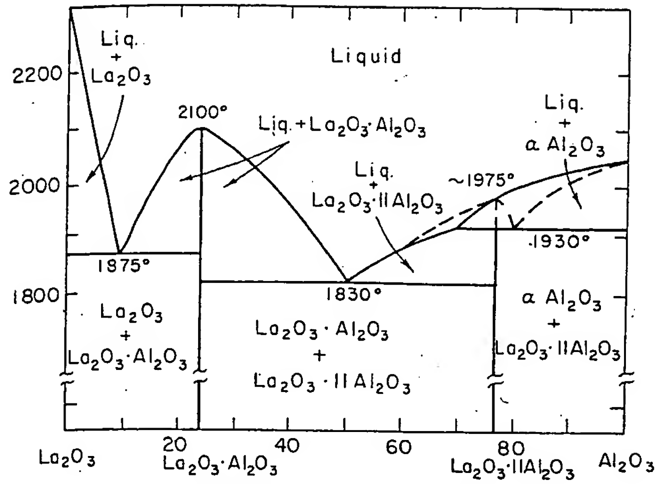

FIG. 2340.—System Al_2O_3–La_2O_3.

I. A. Bondar and N. V. Vinogradova, *Izv. Akad. Nauk SSSR, Ser. Khim.*, No. 5, 785 (1964); Edward T. Fritsche and Lowell G. Tensmeyer, *J. Am. Ceram. Soc.*, 50 [3] 167 (1967), also report an $La_2O_3 \cdot 11Al_2O_3$ compound that melts congruently at 1995°C.

Al_2O_3–Nd_2O_3

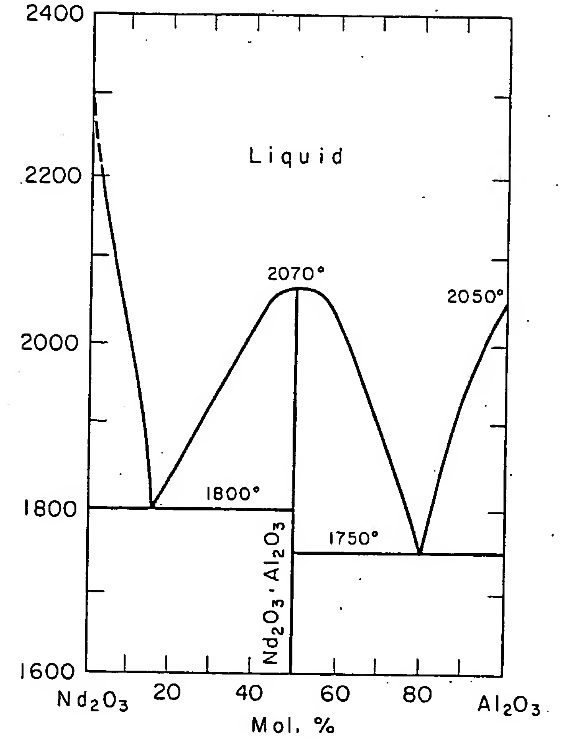

FIG. 2342.—System Al_2O_3–Nd_2O_3.

N. A. Toropov and T. P. Kiseleva, *Zh. Neorgan. Khim.*, 6 [10] 2353 (1961); *Russ. J. Inorg. Chem.* (*English Transl.*), 1193 (1961).

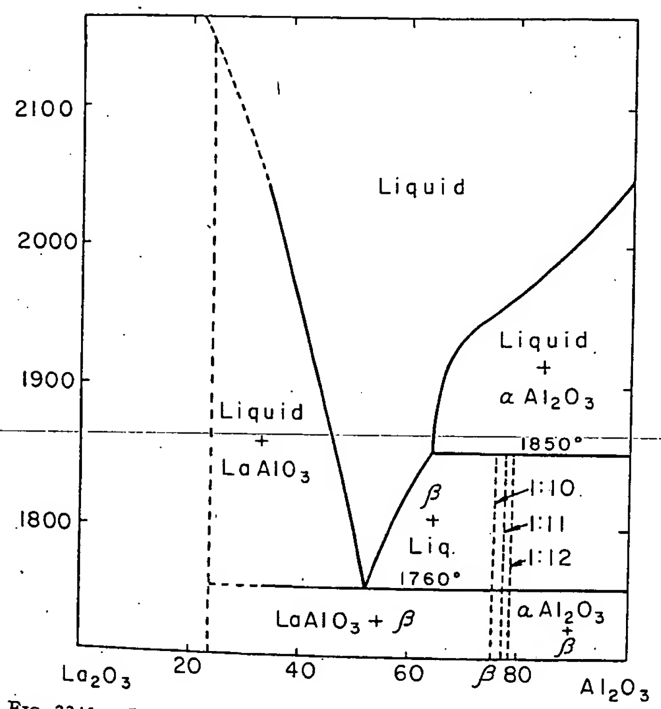

FIG. 2341.—System Al_2O_3–$LaAlO_3$. Compound composition of β is in the range $Na_2O \cdot 10Al_2O_3$ (1:10) to $Na_2O \cdot 12Al_2O_3$ (1:12).

Pham Huu Thanh; Ph.D. Thesis, Sci. Faculty Univ. of Lyon, June, 1965; p. 77 (Order No. 357); Maurice Rolin and Pham Huu Thanh, *Rev. Hautes Temp. Refractaires*, 2 [2] 184 (1965).

Al_2O_3–Sc_2O_3

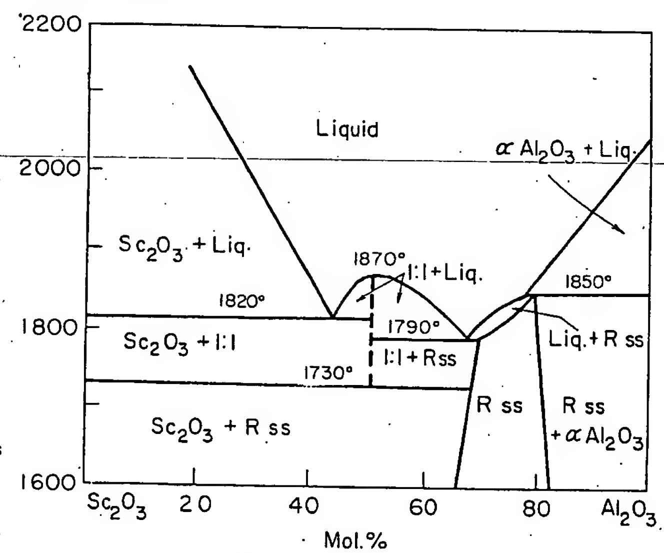

FIG. 2343.—System Al_2O_3–Sc_2O_3. R ss = solid solution phase.

N. A. Toropov and V. A. Vasil'eva, *Dokl. Akad. Nauk SSSR*, 152 [6] 1379 (1963).

Al_2O_3–Y_2O_3

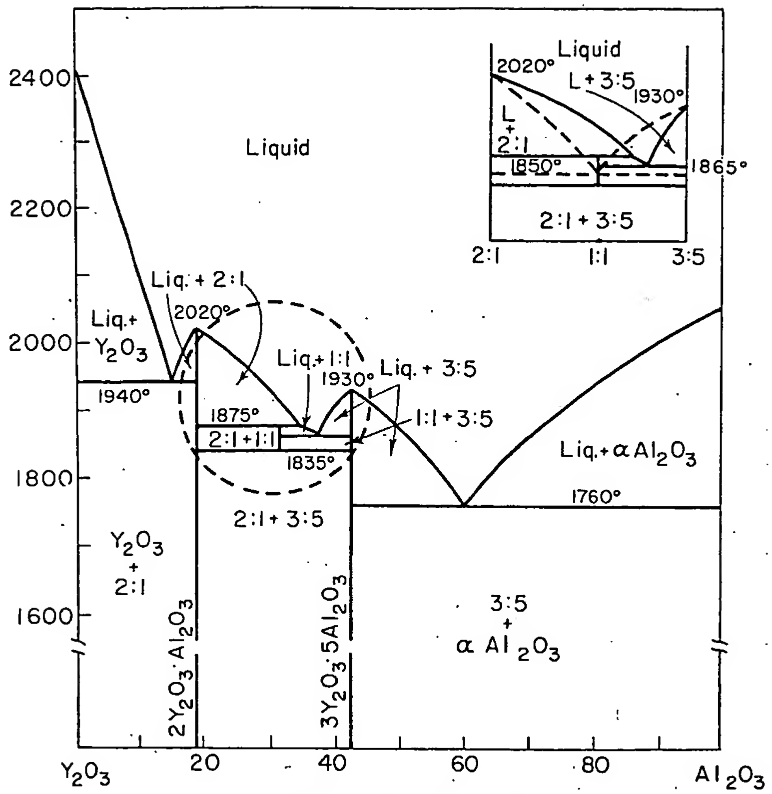

FIG. 2344.—System Al_2O_3–Y_2O_3.

N. A. Toropov, I. A. Bondar, F. Ya. Galakhov, X. S. Nikogosyan, and N. V. Vinogradova, *Izv. Akad. Nauk SSSR, Ser. Khim.*, No. 7, 1162 (1964).

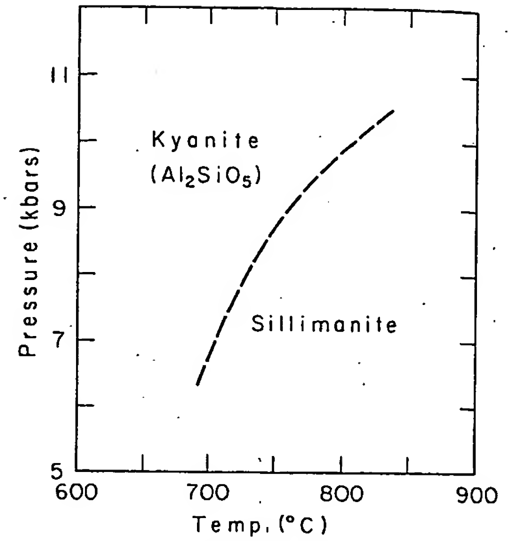

FIG. 2346.—System Al_2SiO_5 showing kyanite-sillimanite equilibrium boundary; tentative.

S. W. Richardson, P. M. Bell, and M. C. Gilbert, *Carnegie Inst. Washington, Yearbook*, 65, 248 (1966).

Al_2O_3–SiO_2

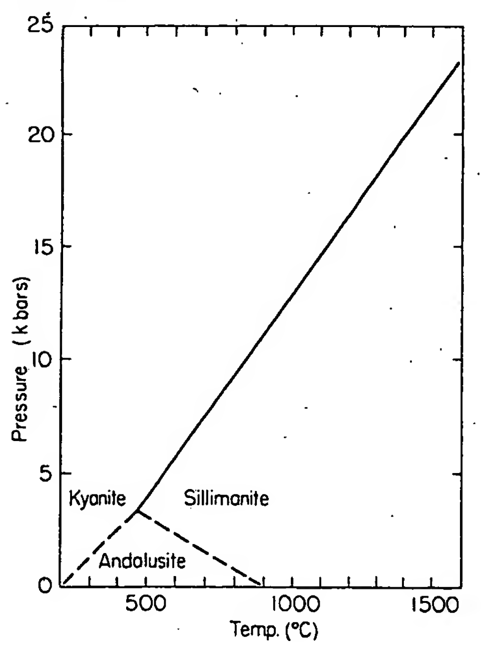

FIG. 2345.—P-T diagram for the system Al_2SiO_5. Kyanite-sillimanite inversion was accomplished hydrothermally.

R. C. Newton, *Science*, 151 [3715] 1223 (1966).

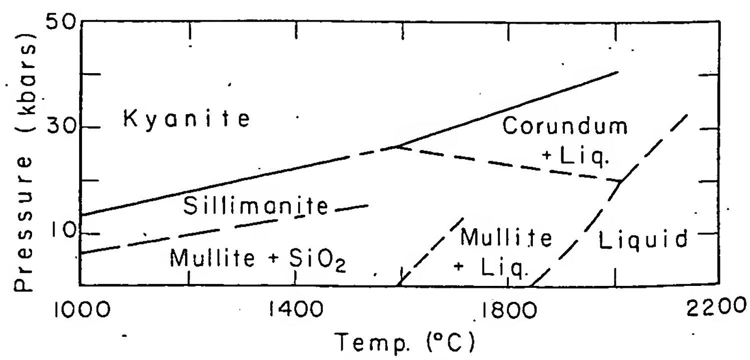

FIG. 2347.—System Al_2O_3–SiO_2 at high temperatures and pressures; deduced.

R. C. DeVries, *J. Am. Ceram. Soc.*, 47 [5] 236 (1964).

Cr_2O_3–Nd_2O_3

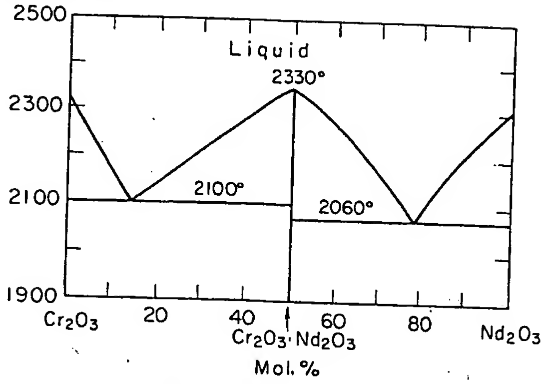

FIG. 2361.—System Cr_2O_3–Nd_2O_3.

V. N. Pavlikov and S. G. Tresvyatskii, *Zh. Neorgan. Khim.*, 11 [6] 1442 (1966); *Russ. J. Inorg. Chem. (English Transl.)*, 771 (1966).

Dy_2O_3–SiO_2

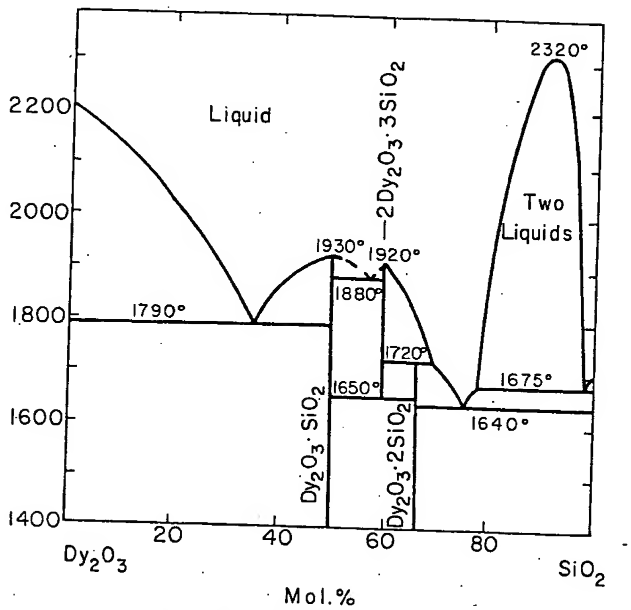

FIG. 2362.—System Dy_2O_3–SiO_2.

N. A. Toropov, F. Ya. Galakhov, and S. F. Konovalova, *Izv. Akad. Nauk SSSR, Ser. Khim.* No. 8, 1368 (1961); *Bull. Acad. Sci. USSR, Div. Chem. Sci. (English Transl.)*, 1275 (1961).

Dy_2O_3–ZrO_2

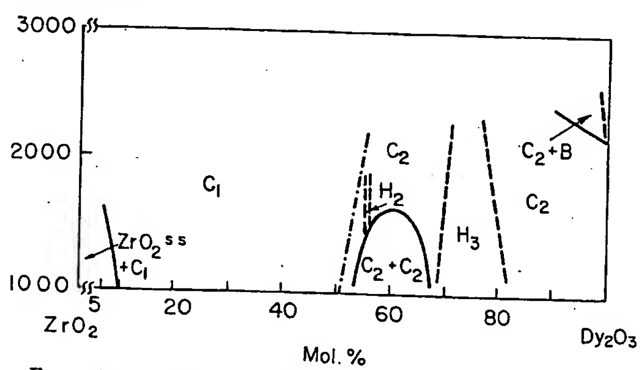

FIG. 2363.—System Dy_2O_3–ZrO_2, subsolidus; proposed. B = rare-earth oxide type, C_1 and C_2 = cubic phases, and H_2 and H_3 = hexagonal phases.

Monique Perez y Jorba, *Ann. Chim. (Paris)*, 7, 509 (1962).

Dy_2O_3–V_2O_5

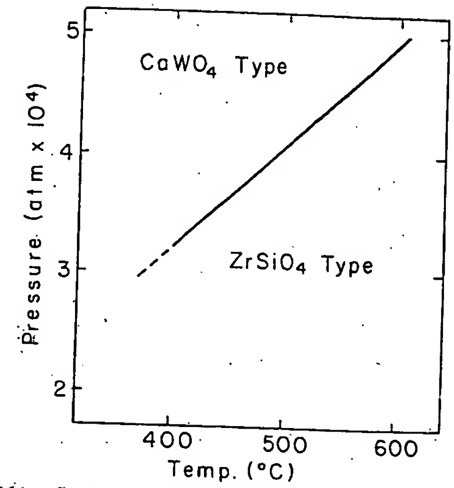

FIG. 2364.—System $DyVO_4$ showing univariant P-T curve for the transition: zircon-type ⇄ scheelite-type structure.

V. S. Stubican and Rustum Roy, *J. Appl. Phys.*, 34 [7] 1888 (1963).

Er_2O_3–SiO_2

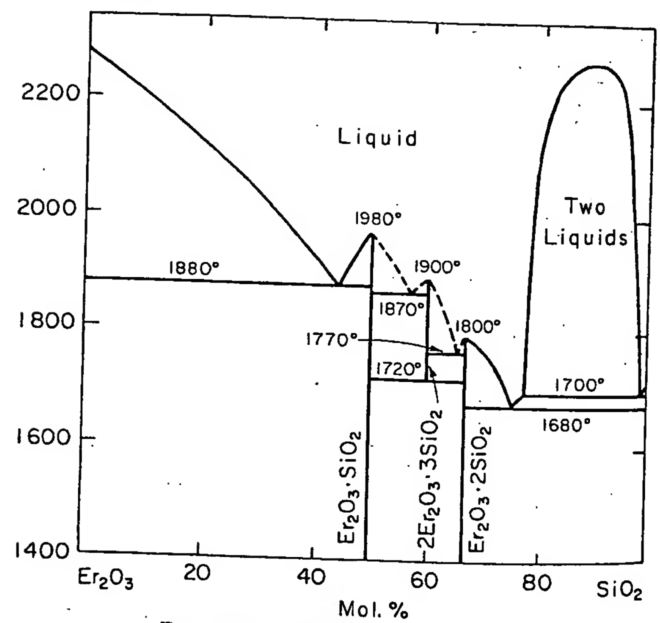

FIG. 2365.—System Er_2O_3–SiO_2.

N. A. Toropov, F. Ya. Galakhov, and S. F. Konovalova, *Izv. Akad. Nauk SSSR, Ser. Khim.*, No. 8, 1370 (1961); *Bull. Acad. Sci. USSR, Div. Chem. Sci. (English Transl.)*, 1275 (1961).

Ga_2O_3–SiO_2

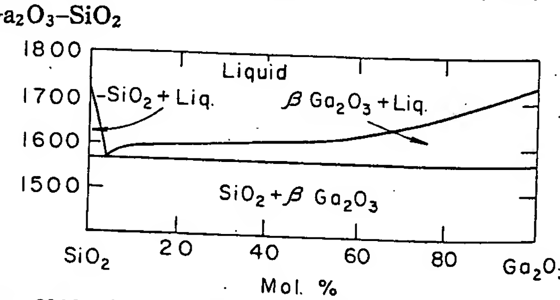

FIG. 2366.—System Ga_2O_3–SiO_2. See Fig. 341 for diagram showing liquid immiscibility.

N. A. Toropov, *Trans. Intern. Ceram. Congr., 7th, London*, 1960, p. 437.

Gd_2O_3–ZrO_2 (concl.)

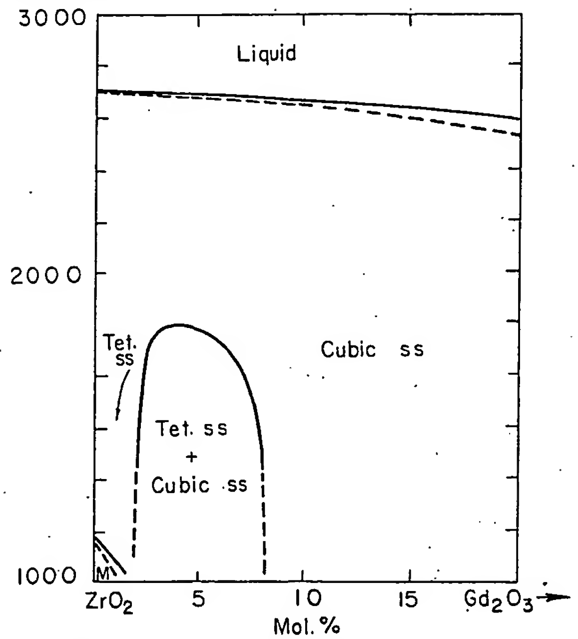

FIG. 2370.—System ZrO_2–Gd_2O_3 showing monoclinic (M) → tetragonal (tet) inversion of ZrO_2.

Jean Lefèvre, *Ann. Chim. (Paris)*, 8 [1–2] 128 (1963).

La_2O_3–HfO_2

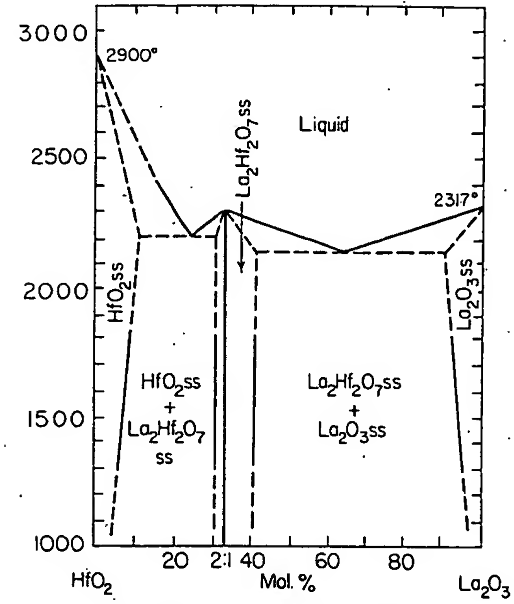

FIG. 2371.—System La_2O_3–HfO_2.

L. N. Komissarova, Wang Kên-shih, V. I. Spitsyn, and Yu. P. Simanov, *Zh. Neorgan. Khim.*, 9 [3] 693 (1964); *Russ. J. Inorg. Chem. (English Transl.)*, 385 (1964).

La_2O_3–SiO_2

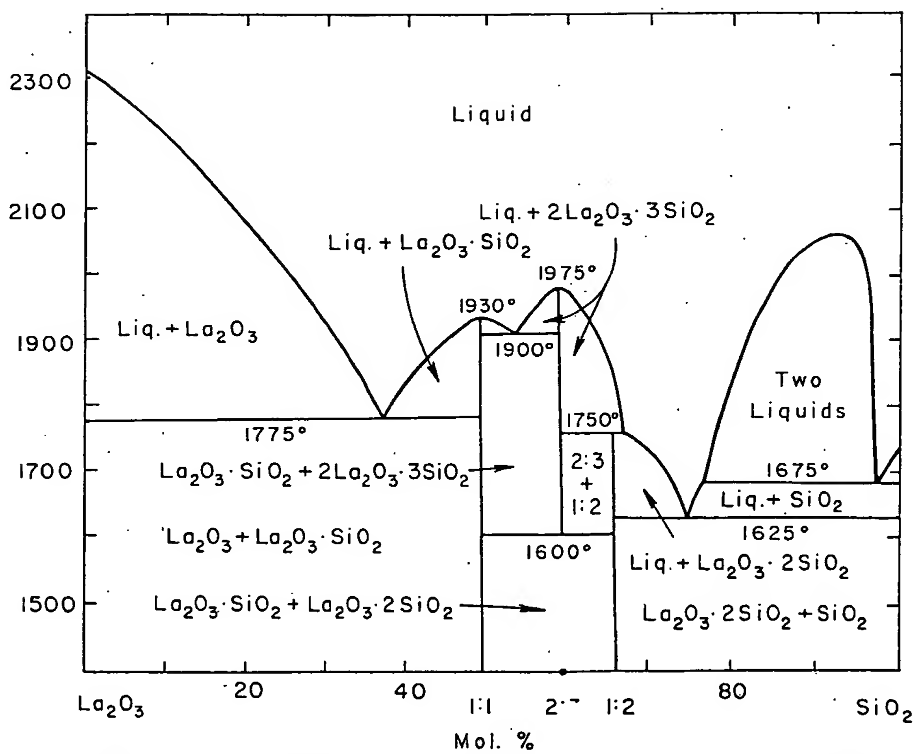

FIG. 2372.—System La_2O_3–SiO_2. Oxide ratios of compounds are given as La_2O_3:SiO_2.

N. A. Toropov, I. A. Bondar, and F. Ya. Galakhov, *Trans. Intern. Ceram. Congr., 8th, Copenhagen*, 1962, p. 87; N. A. Toropov and I. A. Bondar, *Izv. Akad. Nauk SSSR, Otd. Khim. Nauk*, 5, 740 (1961).

La_2O_3–TiO_2

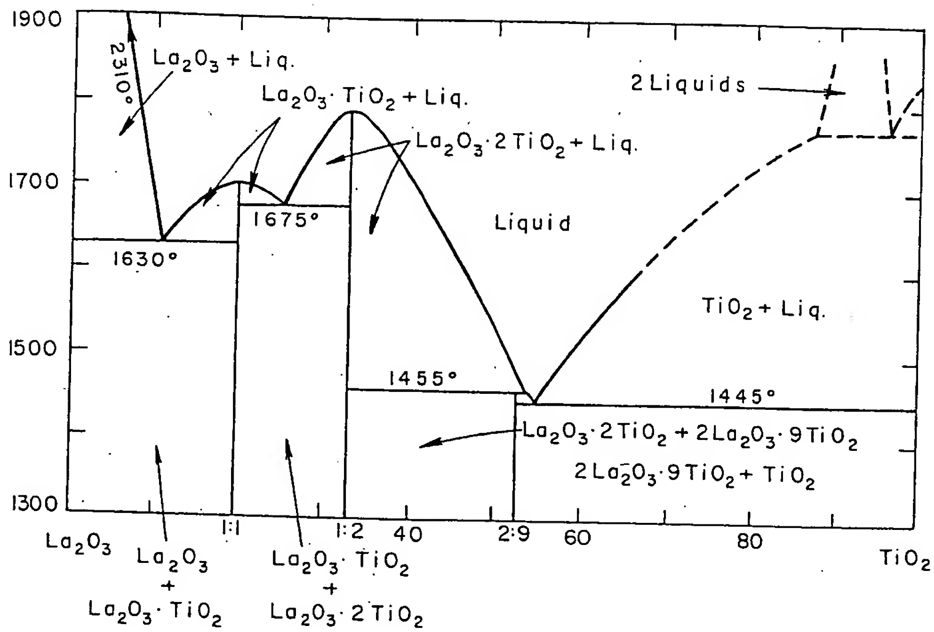

FIG. 2373.—System La_2O_3–TiO_2.

J. B. MacChesney and H. A. Sauer, *J. Am. Ceram. Soc.*, **45** [9] 419 (1962).

La_2O_3–ZrO_2

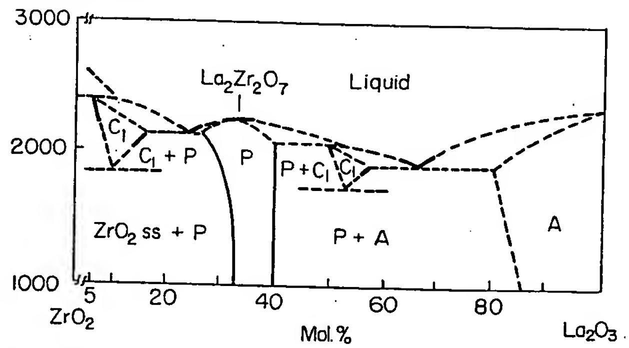

FIG. 2374.—System La_2O_3–ZrO_2; proposed. A = rare-earth oxide type, C_1 = cubic phase, and P = cubic pyrochlore phase.

Monique Perez y Jorba, *Ann. Chim.* (*Paris*), **7**, 509 (1962).

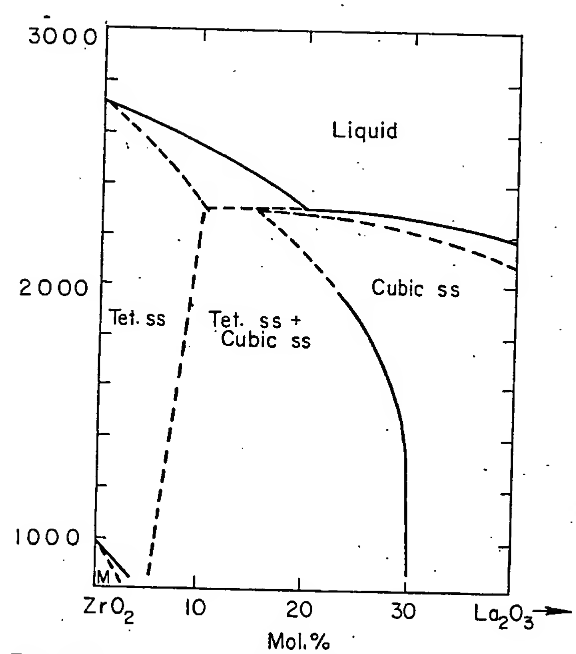

FIG. 2375.—System ZrO_2–La_2O_3 showing monoclinic (M) → tetragonal (tet) inversion of ZrO_2.

Jean Lefèvre, *Ann. Chim.* (*Paris*), **8** [1–2] 128 (1963).

Ln_2O_3–As_2O_5

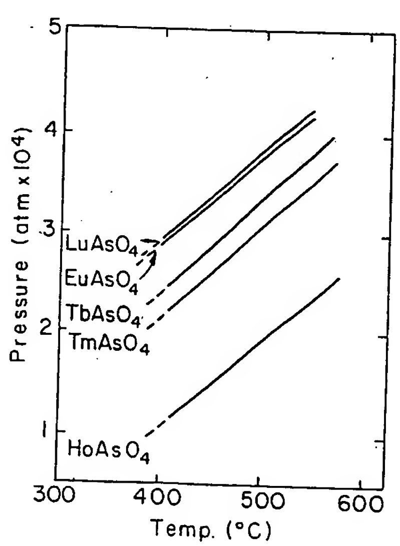

FIG. 2376.—System $LnAsO_4$ showing univariant P-T curves for the transition: zircon-type ⇄ scheelite-type structure for rare-earth atoms with odd atomic numbers.

V. S. Stubican and Rustum Roy, *J. Appl. Phys.*, **34** [7] 1888 (1963).

Nd_2O_3–SiO_2 (concl.)

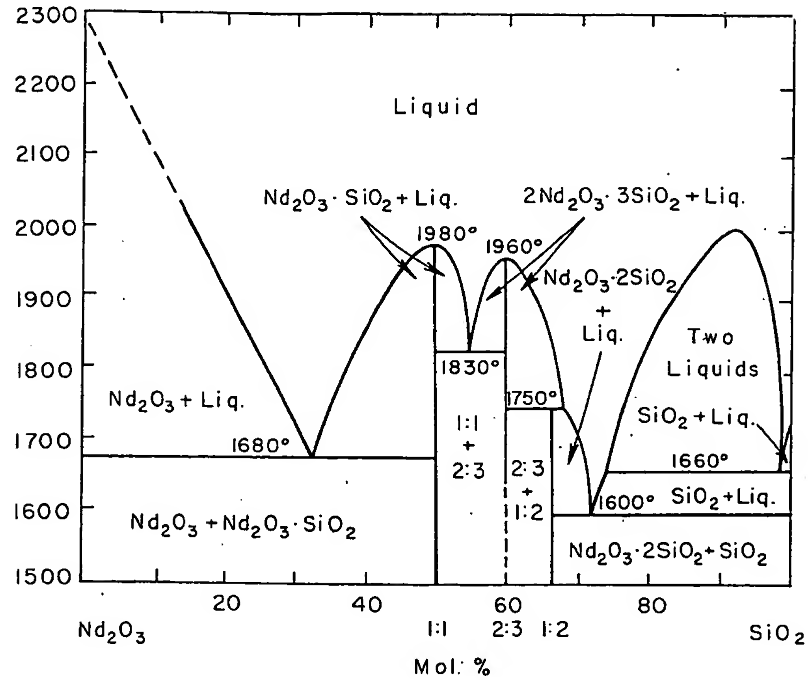

FIG. 2381.—System Nd_2O_3–SiO_2. Oxide ratios of compounds are given as Nd_2O_3:SiO_2.

N. A. Toropov, *Trans. Intern. Ceram. Congr., 7th, London*, 1960, p. 440.

Nd_2O_3–ZrO_2

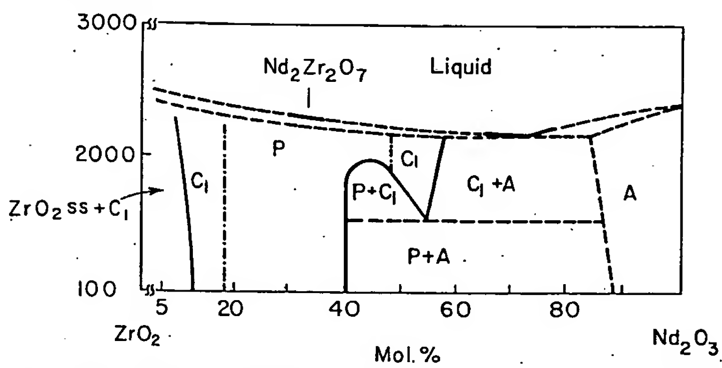

FIG. 2382.—System Nd_2O_3–ZrO_2; proposed. A = rare-earth oxide type, C_I = cubic phase, and P = cubic pyrochlore phase.

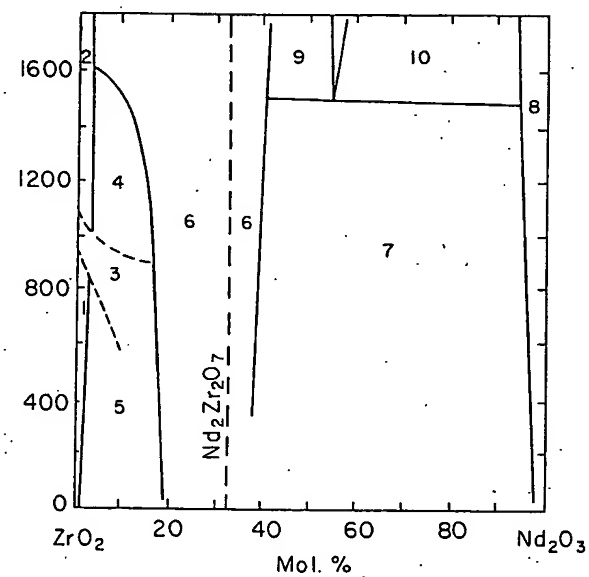

FIG. 2383.—System Nd_2O_3–ZrO_2 showing phase transformations. 1 = monoclinic ss based on ZrO_2, 2 = tetragonal ss based on ZrO_2, 3 = monoclinic ss + tetragonal ss + cubic ss, 4 = tetragonal ss + cubic ss, 5 = monoclinic ss + cubic ss of pyrochlore type, 6 = cubic ss of the pyrochlore type, 7 = cubic ss of the pyrochlore type + tetragonal ss based on neodymium oxide, 8 = hexagonal ss based on neodymium oxide, 9 = cubic (Mn_2O_3 type) ss + cubic (pyrochlore type) ss, and 10 = cubic (Mn_2O_3 type) ss + hexagonal ss.

V. B. Glushkova, I. A. Davtyan, and É. K. Keler, *Izv. Akad. Nauk SSSR, Neorgan. Materialy*, 1 [11] 1955 (1965); *Russ. J. Inorg. Materials (English Transl.)*, 1772 (1965).

Sc_2O_3–SiO_2

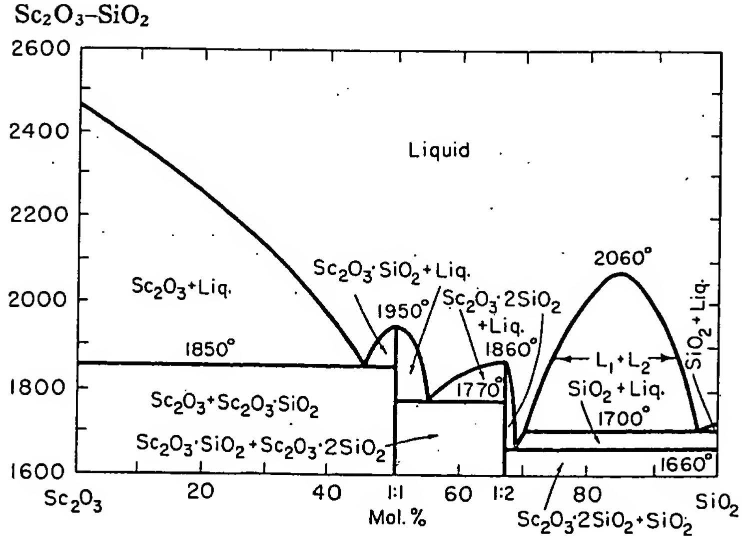

FIG. 2384.—System Sc_2O_3–SiO_2.

N. A. Toropov and V. A. Vasil'eva, *Zh. Neorgan. Khim.*, 7 [8] 1938 (1962); *Russ. J. Inorg. Chem. (English Transl.)*, 1002 (1962).

Sc_2O_3–ZrO_2

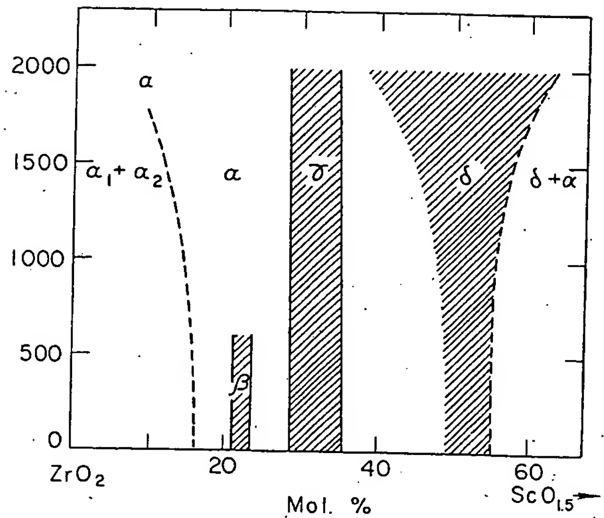

FIG. 2385.—System $ScO_{1.5}$–ZrO_2; subsolidus.

Jean Lefèvre, *Ann. Chim.* (*Paris*), 8 [1–2] 138 (1963).

Sm_2O_3–SiO_2

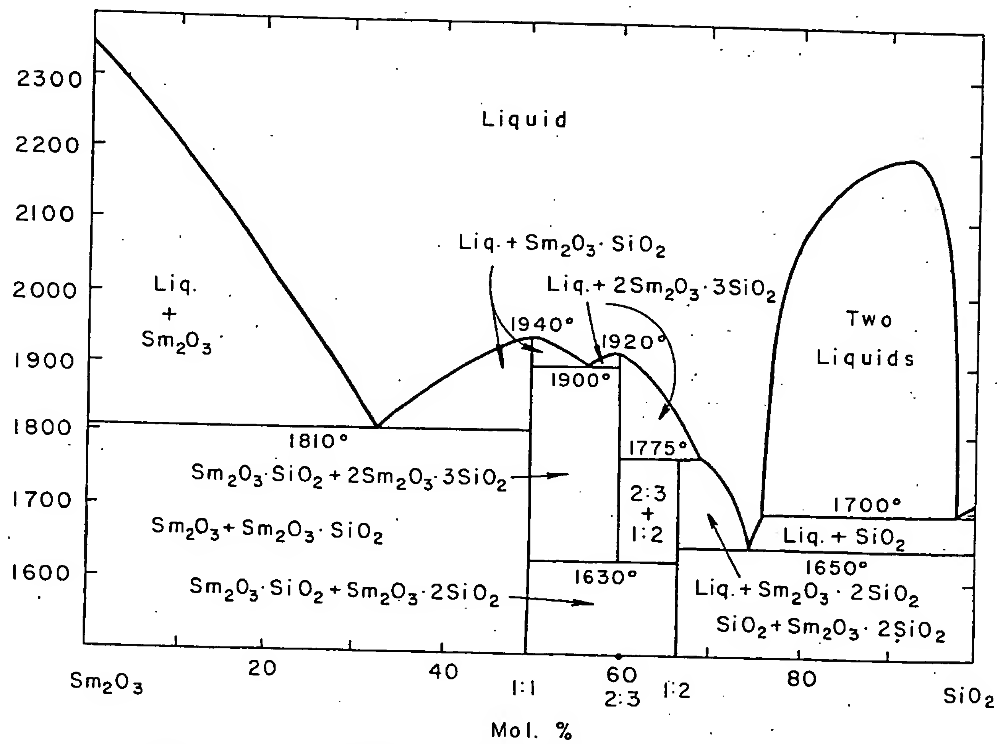

FIG. 2386.—System Sm_2O_3–SiO_2. Oxide ratios of compounds given as Sm_2O_3:SiO_2.

N. A. Toropov, *Trans. Intern. Ceram. Congr., 7th London*, 1960, p. 439; N. A. Toropov and I. A. Bondar, *Izv. Akad. Nauk SSSR, Otd. Khim. Nauk*, No. 8, 1372 (1961); *Bull. Acad. Sci. USSR, Div. Chem. Sci.* (*English Transl.*), 1279 (1961).

Sm_2O_3–ZrO_2

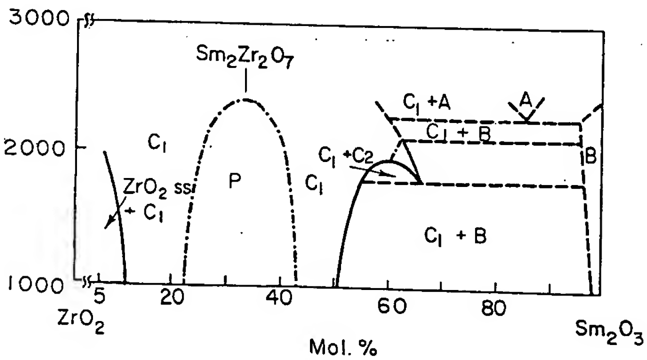

FIG. 2387.—System Sm_2O_3–ZrO_2, subsolidus; proposed. A and B = rare-earth oxide types, C_1 and C_2 = cubic phase, and P = cubic pyrochlore phase.

Monique Perez y Jorba, *Ann. Chim.* (*Paris*), 7, 509 (1962).

Y_2O_3–SiO_2

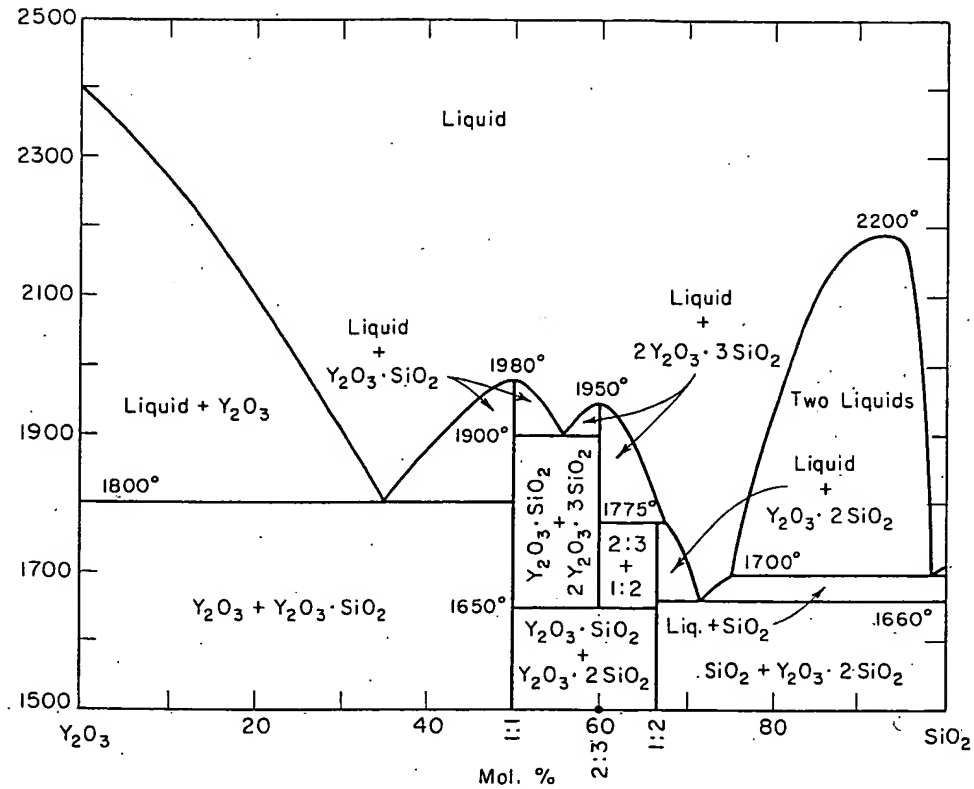

FIG. 2388.—System Y_2O_3–SiO_2. Oxide ratios of compounds are given as Y_2O_3:SiO_2.

N. A. Toropov, *Trans. Intern. Ceram. Congr., 7th, London,* 1960, p. 438; N. A. Toropov and I. A. Bondar, *Izv. Akad. Nauk SSSR, Otd. Khim. Nauk,* 4, 547 (1961).

Y_2O_3–ThO_2

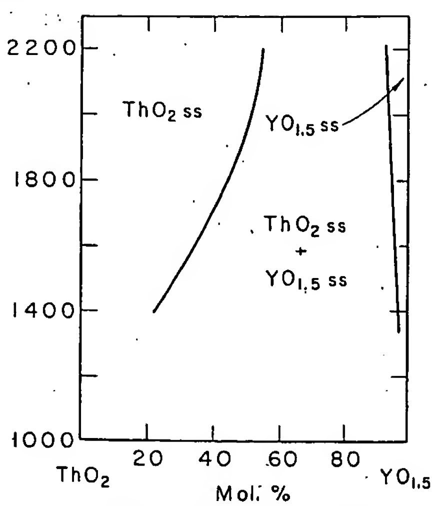

FIG. 2389.—System $YO_{1.5}$–ThO_2.

E. C. Subbarao, P. H. Sutter, and J. Hrizo, *J. Am. Ceram. Soc.,* 48 [9] 445 (1965).

Y_2O_3–ZrO_2

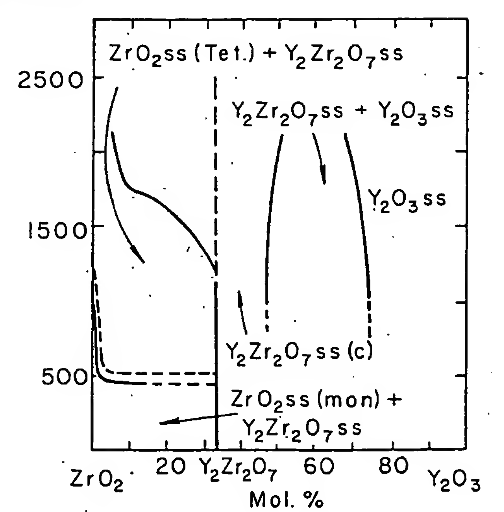

FIG. 2390.—System Y_2O_3–ZrO_2 showing compound $Y_2Zr_2O_7$. c = cubic, mon = monoclinic, and tet = tetragonal.

F. Fu-kang, A. K. Kuznetsov, and E. K. Keler, *Izv. Akad. Nauk SSSR, Otd. Khim. Nauk,* No. 4, 601 (1963).

Yb_2O_3–SiO_2

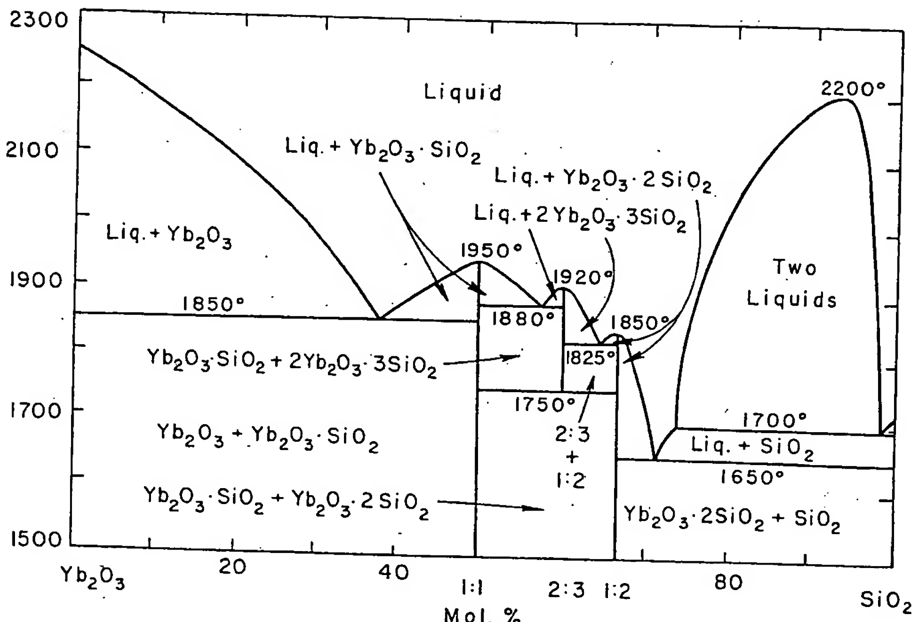

FIG. 2391.—System Yb_2O_3–SiO_2. Oxide ratios of compounds given as Yb_2O_3:SiO_2.

N. A. Toropov, I. A. Bondar, and F. Ya. Galakhov, *Trans. Intern. Ceram. Congr., 8th Copenhagen*, 1962, p. 87; N. A. Toropov and I. A. Bondar, *Izv. Akad. Nauk SSSR, Otd. Khim. Nauk*, No. 8, 1372 (1961); *Bull. Acad. Sci. USSR, Div. Chem. Sci.* (*English Transl.*), 1280 (1961).

Yb_2O_3–ZrO_2

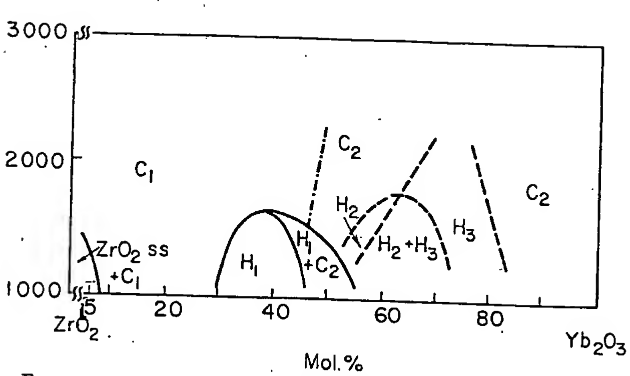

FIG. 2392.—System Yb_2O_3–ZrO_2, subsolidus; proposed. C_1 and C_2 = cubic phases, H_1 = rhombohedral phase, and H_2 and H_3 = hexagonal phases.

Monique Perez y Jorba, *Ann. Chim.* (*Paris*), 7, 509 (1962).

GeO_2–SiO_2

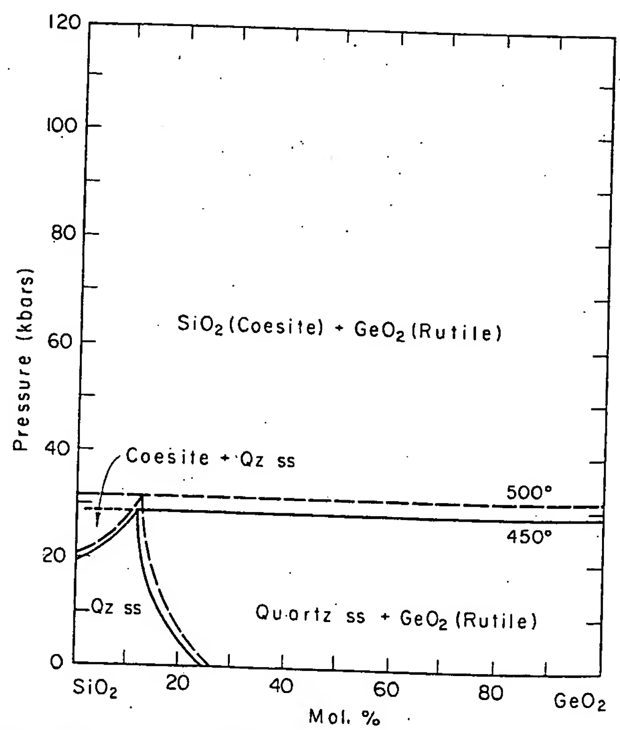

FIG. 2393.—System SiO_2–GeO_2 showing pressure-composition diagrams at 450°C (solid line) and 500°C (dashed line).

W. S. Miller, F. Dachille, E. C. Shafer, and Rustum Roy, *Am. Mineralogist*, 48, 1027 (1963).